Critical current from surface barriers in type-II superconducting strips

Maamar Benkraouda
Physics Department, UAE University, P.O. Box 17551 Al-Ain, United Arab Emirates

John R. Clem
Ames Laboratory and Department of Physics and Astronomy, Iowa State University, Ames, Iowa 50011
(Received 17 August 1998)

Extending a model we previously used to calculate magnetization hysteresis arising from the geometrical barrier in a flat, bulk-pinning-free type-II superconducting strip subjected to a perpendicular magnetic field H_a, we here calculate the contribution, arising from screening currents on the top and bottom surfaces, to the magnetic-field-dependent critical current $I_c(H_a)$ due to surface barriers, including both the geometrical barrier and the Bean-Livingston barrier. [S0163-1829(98)04946-7]

I. INTRODUCTION

A barrier of geometrical origin has been shown[1–3] to delay the first penetration of magnetic flux into a flat type-II superconducting strip subjected to a perpendicular magnetic field. A consequence of this effect is that such a strip exhibits hysteretic behavior even if the vortices in the interior of the strip are completely unpinned, i.e., even if the bulk critical current density J_c is zero. The geometrical barrier is due solely to the nonellipticity of the sample's cross section; it is similar to the barrier observed in type-I superconductors of rectangular cross section,[4] but is different from the Bean-Livingston surface barrier observed in type-II superconductors.[5–11]

In Ref. 12, we introduced a model of a superconducting strip, one flat in the middle and rounded at the edges, to use in approximating the magnetic-field and current-density distributions produced in the range of low perpendicular applied magnetic fields H_a when the geometrical barrier plays a significant role. Several results of our analytical approach have been confirmed independently by numerical calculations.[13–15] In the present paper, we extend the calculations of Ref. 12 to compute the critical current $I_c(H_a)$ due to both geometrical and Bean-Livingston barriers, to which we will refer collectively as surface barriers.

As shown in Refs. 2, 3, and 12, when the applied field is large enough, there is a range of applied fields for which vortices are present in the strip, producing a domelike magnetic field distribution. In the absence of a Bean-Livingston barrier, when H_a is equal to the critical entry field H_{en}, vortices enter the sample until the net magnetic field at the edge of the strip (the sum of the Meissner response to the applied field and the return field arising from vortices inside the sample) is equal to the lower critical field H_{c1}. If the applied field is now reduced slightly, no vortices leave the sample, but the domelike vortex-generated magnetic field distribution changes shape. The height of the dome decreases and the outermost boundaries expand, maintaining constant area (constant magnetic flux) under the dome. When H_a is reduced to the critical exit field H_{ex} at which the outermost boundaries of the dome reach the curved edges of the strip, vortices exit from the strip. Similar behavior is also expected when a Bean-Livingston barrier is present. Moreover, the Bean-Livingston barrier, when present, is expected to be seen over a wider range of applied magnetic fields, possibly up to the bulk thermodynamic critical field H_c.

In applying the above model, we find here that the physics of the critical current $I_c(H_a)$ depends upon the value of the applied field H_a. For small values of H_a, we find that the critical current is just that for which the net field at the left edge of the strip (the sum of the self-field from the current and the Meissner response to the applied field) is equal to H_{c1} in the absence of a Bean-Livingston barrier[5–11] or H_b, the Bean-Livingston barrier field, in the presence of such a barrier. As soon as any vortex is nucleated and moves away from the rounded left edge of the strip, it is swept completely across to the right-hand side of the strip, where it annihilates with its image. For larger values of H_a, there is a domelike magnetic-field distribution produced by vortices inside the strip. The field distribution in the dome is similar to that in the absence of the current, but the dome is shifted to the right because of the Lorentz force from the applied current. The critical current $I_c(H_a)$ is determined chiefly by two critical conditions: first, that the net field at the left edge of the strip (the sum of the self-field from the current, the Meissner response to the applied field, and the return field arising from vortices inside the sample) be equal to H_s and, second, that the right-hand boundary of the dome just reach the rounded edge. Here, H_s is equal to the lower critical field H_{c1} in the absence of a Bean-Livingston barrier or to H_b, the Bean-Livingston barrier field, in the presence of such a barrier. The first of these two critical conditions is that for entry of new vortices at the left edge of the strip, and the second is that for exit (or annihilation) of vortices at the right edge of the strip.

In this paper, we focus on calculating the contribution to the critical current arising from screening currents carried on the top and bottom surfaces of the strip in vortex-free regions. As we shall show in Sec. III, in the field range of interest ($H_a < H_s/2$), this contribution to the current is of order $2\pi W H_s/R$, where $2W$ is the width of the strip, d is the thickness, and $R=(2W/d)^{1/2}$ is the square root of the aspect ratio. In the presence of a surface barrier, however, there will be additional contributions to the current density $\mathbf{J}=\nabla\times\mathbf{H}$ localized at the sample edges. As can be shown using Am-

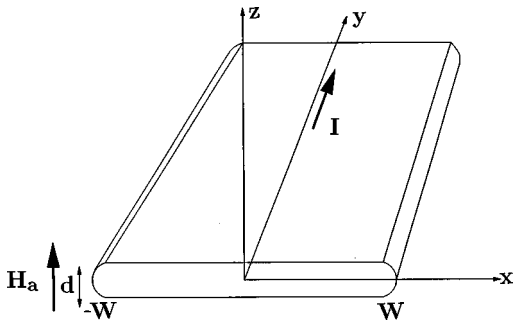

FIG. 1. Sketch of the model superconducting strip considered in this paper. The strip has width $2W$, thickness d, and rounded edges.

père's law, these edge currents contribute a total current of order dH_s, which is smaller by a factor of $1/R$ than the contribution from the top and bottom surfaces in fields less than $H_s/2$. We consider in this paper only the case of large aspect ratios and values of $R \gg 1$, and thus we ignore the edge-current contribution of order dH_s. At fields greater than $H_s/2$, however, the edge-current contribution dominates, and a more careful treatment of this contribution, not included in this paper, would be needed to determine the critical current and how the total current divides between the left and right edges of the strip.

This paper is organized as follows: In Sec. II we present the equations for the current distributions in the strip due to the applied magnetic field, the applied current, and the flux distribution inside the strip and calculate the field and current distributions in the case of quasistatic flux penetration in a dome is present. In Sec. III we establish the critical conditions for the critical current $I_c(H_a)$ and its dependence on the applied field. In Sec. IV we summarize our results and suggest experiments to test the theory.

II. QUASISTATIC FLUX DISTRIBUTION WHEN A DOME IS PRESENT

We consider an infinite superconducting strip of width $2W(-W<x<W)$, thickness $d \ll W$ (see Fig. 1), and penetration depth $\lambda \leqslant d$. A uniform magnetic field H_a in the z direction and a current I in the y direction are applied. In the Meissner state, where no flux has penetrated the strip, the current density distribution, averaged over the thickness d of the strip, is given by[16,17]

$$J_{My}(x) = -\frac{2H_a x}{d\sqrt{W^2-x^2}} + \frac{I}{\pi d\sqrt{W^2-x^2}}. \tag{1}$$

When vortices are present in the strip, generating a flux distribution $B_z(x')$, the corresponding current density distribution is given by[12]

$$J_{vy}(x) = \frac{2}{\mu_0 \pi d}\int_{-W}^{W} \frac{B_z(x')\sqrt{W^2-x'^2}}{(x-x')\sqrt{W^2-x^2}}dx'. \tag{2}$$

Let us assume that I and H_a are such that there is a static domelike flux distribution inside the strip. For the vortices to be at rest inside the sample, the total current density distribution must be zero inside the region where the vortices are. Thus the total current density in this region is

$$J_y(x) = J_{My}(x) + J_{vy}(x) = 0. \tag{3}$$

Let the domelike flux distribution extend from a to b, where $a<b$. Then the solution to Eq. (3) is

$$B_z(x) = \begin{cases} B_0 \dfrac{\sqrt{(x-a)(b-x)}}{\sqrt{W^2-x^2}} & \text{for } a<x<b, \\ 0 \quad \text{otherwise,} \end{cases} \tag{4}$$

where B_0 is a constant to be determined below. This flux distribution generates the current density [Eq. (2)]

$$J_{vy}(x) = \frac{B_0}{\mu_0 d}\frac{2x-(a+b)}{\sqrt{W^2-x^2}} \tag{5}$$

in the region $a<x<b$. For $J_{vy}(x)$ to cancel $J_{My}(x)$ [Eq. (1)] in this region and satisfy Eq. (3), we must have

$$B_0 = \mu_0 H_a \tag{6}$$

and

$$I = \pi H_a (a+b). \tag{7}$$

The above equations describe a variety of possible metastable distributions of magnetic flux and current density, all with the same applied magnetic field H_a and current I. Since only the sum of a and b is determined by Eq. (7), the above equations alone are insufficient to determine the positions a and b of the left and right boundaries of the domelike flux distribution of Eq. (4). Because the possible distributions are dependent upon the magnetic history of the sample, it is necessary to supply some additional information to determine the values of a and b uniquely.

We therefore next assume that the sample is at the *critical entry condition*. That is, if $I=0$, the applied field ($H_a>0$) is such that the local magnetic fields at the left and right edges of the sample (H_{left} and H_{right}) are both equal to H_s, so that vortices either have just entered the sample or are on the verge of doing so. If $I>0$, the self-field from the current is positive on the left side of the sample and negative on the right, such that $H_{left}>H_{right}>0$, and the critical entry condition is reached only on the left edge of the sample. Using the procedure for calculating the fields on the rounded edges of the sample described in Refs. 10 and 11, we obtain

$$H_{left} = H_a(R+1) + \frac{IR}{2\pi W} - \frac{H_a R}{\pi W}\int_a^b \frac{\sqrt{(x-a)(b-x)}}{W+x}dx, \tag{8}$$

$$H_{right} = H_a(R+1) - \frac{IR}{2\pi W} - \frac{H_a R}{\pi W}\int_a^b \frac{\sqrt{(x-a)(b-x)}}{W-x}dx, \tag{9}$$

where $R=\sqrt{2W/d}$. Performing the required integrals, we obtain

$$H_{left} = H_a[1 + R\sqrt{(1+a/W)(1+b/W)}], \tag{10}$$

$$H_{right} = H_a[1 + R\sqrt{(1-a/W)(1-b/W)}]. \tag{11}$$

Using the critical entry condition at the left edge, $H_{left} = H_s$, we obtain

$$H_s = H_a[1 + R\sqrt{(1+a/W)(1+b/W)}], \tag{12}$$

which, together with Eq. (7), uniquely determines a and b at the critical entry condition for given H_a and I:

$$a_{en} = W\left[\frac{I}{2\pi W H_a} - \sqrt{\left(1+\frac{I}{2\pi W H_a}\right)^2 - \left(\frac{H_s - H_a}{R H_a}\right)^2}\right], \tag{13}$$

$$b_{en} = W\left[\frac{I}{2\pi W H_a} + \sqrt{\left(1+\frac{I}{2\pi W H_a}\right)^2 - \left(\frac{H_s - H_a}{R H_a}\right)^2}\right]. \tag{14}$$

The total current density, determined by evaluating the integral obtained by substituting Eq. (4) into Eq. (2) and combining the result with Eq. (1), is

$$J_y(x) = \begin{cases} \dfrac{2H_a}{d}\dfrac{\sqrt{(b-x)(a-x)}}{\sqrt{W^2-x^2}} & \text{for } -W<x<a, \\ 0 \quad \text{for } a<x<b, \\ -\dfrac{2H_a}{d}\dfrac{\sqrt{(x-b)(x-a)}}{\sqrt{W^2-x^2}} & \text{for } b<x<W. \end{cases} \tag{15}$$

With a, b, and B_0 determined by Eqs. (6), (7), and (12), we now can calculate the flux distribution $B_z(x)$ [Eq. (4)] and the corresponding current distribution $J_y(x)$ [Eq. (15)] at the critical entry condition for arbitrary values of the applied field H_a and current I. Figures 2(a) and 2(b) show examples of such results for a fixed value of H_a and three values of the current I. For zero current, the domelike flux distribution is centered in the middle of the strip ($a=-b$). As the current increases, the self-field at the left edge causes new vortices to enter the sample, and the center of gravity of the resulting flux distribution shifts to the right. Note that with increasing current, the right boundary of the flux distribution (at $x=b$) approaches the right edge of the strip. We define the critical current I_c as the current that causes vortices at the right boundary of the flux distribution to first reach the rounded edge of the strip.

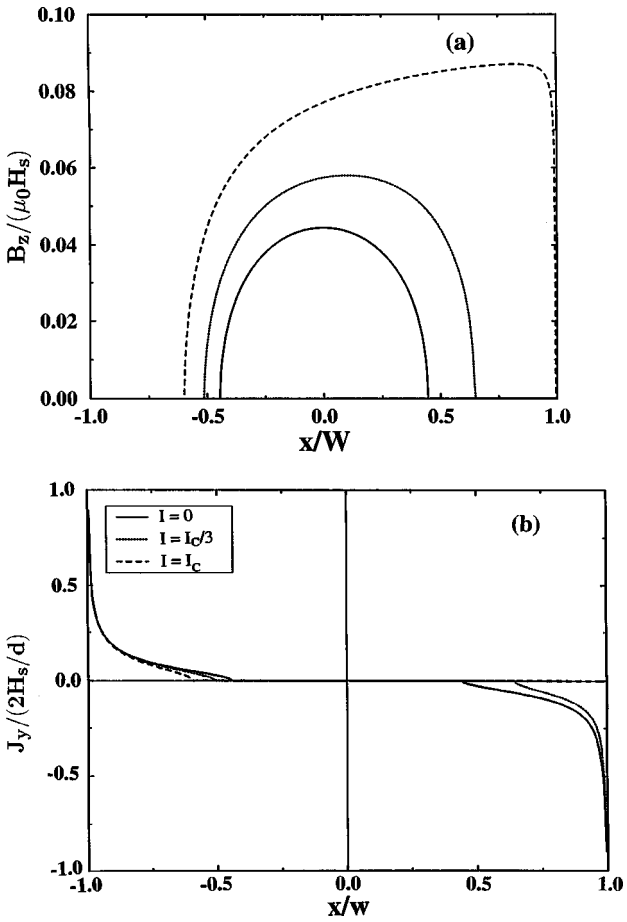

FIG. 2. (a) Flux-density profiles B_z vs x [Eq. (4)] for initial penetration of magnetic flux (critical entry condition at the left side of the strip) in an applied field $H_a = H_s/10$ for an applied current I initially equal to zero, and then at higher currents $I_c/3$ and I_c, the critical current (critical exit condition at the right side of the strip), for $R=(2W/d)^{1/2}=10.05$. (b) Corresponding current-density profiles J_y vs x [Eq. (15)].

III. CRITICAL CURRENT

A. With a dome

Because of the surface barrier, a domelike magnetic-flux distribution occurs in flat strips for a range of applied fields H_a depending upon the current I. In Sec. II, we derived expressions that determine the boundaries $x=a$ and b of the dome at the critical entry condition, for which $H_{left}=H_s$. When $I=0$, the metastable dome (with $a=-b$) occurs for applied fields H_a in the range[12]

$$H_s/(R+1) < H_a < H_s/2, \tag{16}$$

where $R=(2W/d)^{1/2}$ and we have neglected terms of order H_s/R^2. At the lower limit, $b=a=0$, and the field $H_s/(R+1)$ is the value of H_a at which the first vortex enters the strip. At the upper limit, $b=-a=W-d/4$. For $H_a > H_s/2$, there is no further magnetic irreversibility due to the surface barrier (associated with currents flowing on the top and bottom surfaces of the sample), although the Bean-Livingston barrier (associated with currents flowing on the right and left edges of the sample) still can produce irreversibility. However, we neglect the latter contribution in this paper for reasons discussed in Sec. I. We also neglect bulk pinning, another common source of irreversibility.

When $I>0$, the metastable dome occurs for applied fields in the range

$$\frac{H_s}{R+1} - \frac{IR}{2\pi W(R+1)} < H_a < \frac{H_s^2}{2(H_s + IR^2/\pi W)}, \tag{17}$$

where again we neglected terms of order H_s/R^2. At the lower limit, $a=b=I/2\pi H_a$, and the field $H_s/(R+1) - IR/[2\pi W(R+1)]$ is just the value of the applied field at which the net field at the left edge, including the self-field from the current, is equal to H_s. The first entering vortex comes to rest at $x=a=b=I/2\pi H_a < W$. At the upper limit, $b=W-d/4$.

For increasing current, the range of applied fields for which the metastable dome occurs [Eq. (17)] becomes smaller. This range finally vanishes at the current

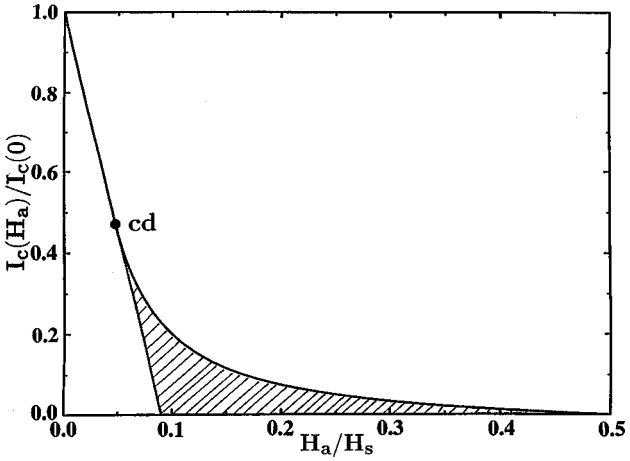

FIG. 3. Critical current I_c, normalized to $I_c(0)=2\pi WH_s/R$, as a function of the applied field $H_a(0<H_a<H_s/2)$ for $R=10.05$ [Eqs. (20) and (22)]. The cross-hatched region indicates the values of H_a and I that produce a domelike flux distribution in the sample, and the point cd marks the point (H_{cd} and I_{cd}) where the dome disappears.

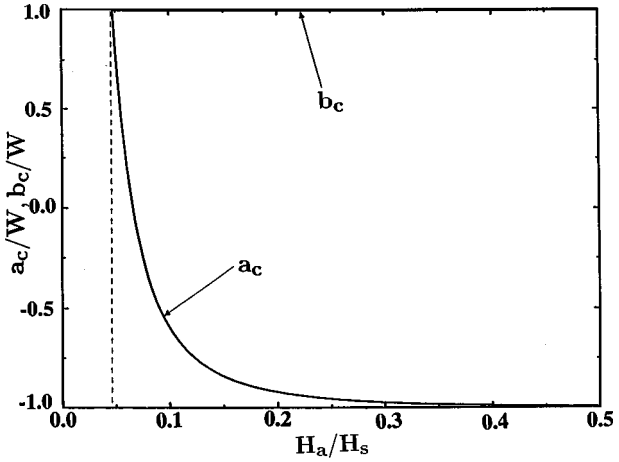

FIG. 4. The coordinates of the left and right boundaries, $x=a_c$ and b_c, respectively, of the domelike flux distribution at the critical current I_c as a function of the applied field H_a. The width of the sample is $2W$, and $R=(2W/d)^{1/2}=10.05$. The vertical dashed line denotes the field $H_a=H_{cd}$, below which the critical dome is absent.

$$I_{cd}=2\pi H_s\frac{W}{2R+1}. \tag{18}$$

At this critical value of the current and at the corresponding critical value of the applied field,

$$H_{cd}=\frac{H_s}{2R+1}, \tag{19}$$

the dome disappears. [In both Eqs. (18) and (19) we have neglected terms of higher order in $1/R$.] Although this combination of current and field produces the critical entry condition ($H_{left}=H_s$), any entering vortex is swept all the way to the right rounded edge ($x=W-d/4$), where it exits from the sample and annihilates with its image.

For currents $I<I_{cd}$, there is a dome present at the critical current I_c, where two conditions are met: a *critical entry condition* at the left side of the sample ($H_{left}=H_s$) and a *critical exit condition* at the right side of the sample ($b=W-d/4$) [see Fig. 2(a) at $I=I_c$]. For any current slightly larger than I_c, new vortices will be nucleated at the left edge of the sample and be driven very rapidly through the otherwise vortex-free region, $-W+d/4<x<a$. These vortices will join the left side of the domelike flux distribution, which will respond by pushing an equal number of vortices out of the dome at $x=W-d/4$, where these vortices will annihilate with their images at the right edge of the sample.

The critical current I_c for applied fields in the range $H_{cd}\leqslant H_a\leqslant H_s/2$ is

$$I_c(H_a)=\frac{\pi WH_s}{R^2}\left(\frac{H_s}{2H_a}-1\right), \tag{20}$$

where we have retained terms only through order $\pi WH_s/R^2$. Note that I_c reduces to zero when $H_a=H_s/2$, and to I_{cd} when $H_a=H_{cd}$. Shown in Fig. 3 is a plot of I_c as a function of the applied field H_a. The crosshatched region indicates the region of the I-H_a plane where a domelike flux distribution occurs with the critical entry condition at the left edge of the sample [see Eq. (17)]. The point cd marks the values of I and H_a where the critical dome shrinks to zero width. Shown in Fig. 4 are the values of a and b, the left and right boundaries of the dome, at the critical current: $a_c=I_c/\pi H_a-b_c$ and $b_c=W-d/4=W(1-1/2R^2)$. Note that $a_c=b_c$ when $H_a=H_{cd}$ and $I=I_{cd}$, while $a_c=-b_c$ when $H_a=H_s/2$ and $I_c=0$.

B. Without a dome

For $H_a<H_{cd}$, there is no metastable dome, and the sample remains in the Meissner state. The critical current in the absence of an applied magnetic field is

$$I_c(0)=2\pi WH_s/R, \tag{21}$$

the current for which the self-field at the edge is H_s [see Eq. (8)]. For small values of the applied magnetic field H_a (i.e., $H_a<H_{cd}$ and $I>I_{cd}$), the critical current is

$$I_c(H_a)=I_c(0)-2\pi WH_a(R+1)/R. \tag{22}$$

For these values of H_a, the Meissner-state current density obeys $J_{My}(x)>0$ for the entire flat region of the strip. Any vortex nucleated at the left edge is thus swept entirely across the sample to the opposite curved edge, where the vortex annihilates with its image. This portion of the $I_c(H_a)$ vs H_a curve is shown in Fig. 3 as the solid straight-line segment from $H_a=0$ and $I_c=I_c(0)$ to $H_a=H_{cd}$ and $I_c=I_{cd}$.

The dotted straight-line extension of the $I_c(H_a)$ line for $H_a>H_{cd}$ and $I<I_{cd}$ is given by

$$I_{c1}(H_a)=I_c(0)-2\pi WH_a(R+1)/R, \tag{23}$$

along which the field at the left edge of the sample is equal to H_s and the rest of the sample is in the Meissner state. For these values of H_a, a current I slightly larger than I_{c1} causes a vortex to nucleate at the left edge, but this vortex comes to rest at a point $x=a=I/2\pi H_a<W$. Even larger currents cause the growth of a domelike flux distribution, as discussed above. The triangular region in the lower left-hand corner of Fig. 3, below the $I_{c1}(H_a)$ line, represents the val-

ues of H_a and I for which the sample remains in the Meissner state and the local field at the edge is less than H_s.

IV. SUMMARY

In this paper we have solved for the critical current due to surface barriers in a flat type-II superconducting strip, when the dominant contribution to the current arises from screening supercurrents in vortex-free regions on the top and bottom surfaces of the strip. By modeling the strip as being flat except at the edges, where it is rounded to elliptical shape with a local radius of curvature equal to half the film thickness, we have derived expressions for the critical current I_c as a function of the applied field H_a. For values of H_a less than H_{cd} [Eq. (19)], the critical current is given by Eq. (22), at which the self-field at the left edge of the sample, taking into account the Meissner response to both the applied field and the current, is equal to H_s.

For $H_a > H_{cd}$, a domelike magnetic-field distribution occurs in the strip [Fig. 2(a)], and the vortices in the sample generate, at the sample's edge, a magnetic field that opposes the local field arising in response to H_a. For currents just below I_c in fields $H_a > H_{cd}$ where a dome is present, there is no net supercurrent flowing where the vortices are, but supercurrents do flow with a high current density in the vortex-free regions on either side of the vortex-filled regions [Fig. 2(b)]. At the critical current I_c, the sample is at the critical entry condition on the left side of the dome and at the critical exit condition on the right side. We have taken into account the return field from vortices in the dome in deriving the dependence of $I_c(H_a)$ as a function of H_a [Eq. (20)].

It has been shown experimentally that the surface barrier makes an important contribution to both the hysteretic magnetization and the transport properties for superconducting strips[10,18–21] over a wide region of the magnetic-field–temperature (H-T) plane. Moreover, in $Bi_2Sr_2CaCu_2O_{8+\delta}$ single crystals, the current density distribution has been found to be concentrated at the edges of the sample when the surface barrier is in effect,[10] in qualitative agreement with our calculations. To provide a more stringent test of the present theory, however, experiments should be done to simultaneously measure the critical current I_c and the magnetic-field profile $B_z(x)$ at the critical current as a function of the applied field H_a. In addition, since the critical current is scaled by the field H_s, measurements of I_c as a function of temperature T also would help to distinguish whether H_s is given by the lower critical field H_{c1} or by a considerably larger barrier field H_b. Under ideal circumstances, H_b could approach the bulk thermodynamic critical field H_c, with a temperature dependence close to $1-(T/T_c)^2$.[5] On the other hand, it is possible that H_b is an effective barrier field determined by matching the time scale of the experiment with the time it takes for vortices to be thermally excited over the surface barrier; in such a case, H_b is expected to be strongly temperature dependent.[22,21]

ACKNOWLEDGMENTS

We thank R. A. Doyle, T. B. Doyle, V. G. Kogan, E. Zeldov, and H. Castro for stimulating comments. Ames Laboratory is operated for the U.S. Department of Energy by Iowa State University under Contract No. W-7405-Eng-82. This research was supported by the Director for Energy Research, Office of Basic Energy Sciences.

[1] M. V. Indenbom, H. Kronmüller, T. W. Li, P. H. Kes, and A. A. Menovsky, Physica C **222**, 203 (1994).
[2] Th. Schuster, M. V. Indenbom, H. Kuhn, E. H. Brandt, and M. Konczykowski, Phys. Rev. Lett. **73**, 1424 (1994).
[3] E. Zeldov, A. I. Larkin, V. B. Geshkenbein, M. Konczykowski, D. Majer, B. Khaykovich, V. M. Vinokur, and H. Shtrikman, Phys. Rev. Lett. **73**, 1428 (1994).
[4] J. Provost, E. Paumier, and A. Fortini, J. Phys. F **4**, 439 (1974).
[5] C. P. Bean and J. D. Livingston, Phys. Rev. Lett. **12**, 14 (1973).
[6] John R. Clem, in *Proceedings of the Conference on Low Temperature Physics* (LT 13), edited by K. D. Timmerhaus, W. J. O'Sullivan, and E. F. Hammel (Plenum, New York, 1974), Vol. 3, p. 102.
[7] J. R. Clem, J. Appl. Phys. **50**, 3518 (1979).
[8] L. Burlachkov, Phys. Rev. B **47**, 8056 (1993).
[9] A. Buzdin and D. Feinberg, Phys. Lett. A **165**, 281 (1992).
[10] D. T. Fuchs, E. Zeldov, M. Rappaport, T. Tamegai, S. Ooi, and H. Shtrikman, Nature (London) **391**, 373 (1998).
[11] D. T. Fuchs, R. A. Doyle, E. Zeldov, D. Majer, W. S. Seow, T. Tamegai, S. Ooi, R. J. Drost, M. Konczykowski, and P. H. Kes, Physica C **282-287**, 2023 (1997).
[12] M. Benkraouda and J. R. Clem, Phys. Rev. B **53**, 5716 (1996).
[13] T. B. Doyle and R. Labusch, J. Low Temp. Phys. **105**, 1207 (1996).
[14] R. Labusch and T. B. Doyle, Physica C **290**, 143 (1997).
[15] T. B. Doyle, R. Labusch, and R. A. Doyle, Physica C **290**, 148 (1997).
[16] J. R. Clem, R. P. Huebener, and D. E. Gallus, J. Low Temp. Phys. **6**, 449 (1973).
[17] E. Zeldov, J. R. Clem, M. McElfresh, and M. Darwin, Phys. Rev. B **49**, 9802 (1994).
[18] N. Chikumoto, M. Konczykowski, N. Motohira, and A. P. Malozemoff, Phys. Rev. Lett. **69**, 1260 (1992).
[19] M. Konczykowski, L. I. Burlachkov, Y. Yeshurun, and F. Holtzberg, Phys. Rev. B **43**, 13 707 (1991).
[20] E. Zeldov, D. Majer, M. Konczykowski, A. I. Larkin, V. M. Vinokur, V. B. Geshkenbein, N. Chikumoto, and H. Shtrikman, Europhys. Lett. **30**, 367 (1995).
[21] L. Burlachkov, A. E. Koshelev, and V. M. Vinokur, Phys. Rev. B **54**, 6750 (1996).
[22] V. N. Kopylov, A. E. Koshelev, I. F. Schegolev, and T. G. Togonidze, Physica C **170**, 291 (1990).